NASA CONTRACTOR REPORT

NASA CR-202

COMPRESSIVE STRENGTH OF BORON-METAL COMPOSITES

by H. Schuerch

Prepared under Contract No. NASw-652 *by*
ASTRO RESEARCH CORPORATION
Santa Barbara, Calif.
for

NATIONAL AERONAUTICS AND SPACE ADMINISTRATION • WASHINGTON, D. C. • APRIL 1965

NASA CR-202

COMPRESSIVE STRENGTH OF BORON-METAL COMPOSITES

By H. Schuerch

Prepared under Contract No. NASw-652 by
ASTRO RESEARCH CORPORATION
Santa Barbara, Calif.

for

NATIONAL AERONAUTICS AND SPACE ADMINISTRATION

For sale by the Office of Technical Services, Department of Commerce,
Washington, D.C. 20230 -- Price $2.00

TABLE OF CONTENTS

LIST OF SYMBOLS

f	stress
F	stress at failure
E	Young's modulus
$\overline{E}$	tangent modulus
G	shear modulus
$\overline{G}$	tangent shear modulus
α	fiber packing density
μ	Poisson's ratio
ε	strain
ρ	specific weight

Subscripts:

c	composite
cr	crippling
sym	symmetrical
antis	antisymmetrical
m	matrix
f	fiber
y	yield
ult	ultimate

SUMMARY

The compressive strength and failure mechanisms of an idealized composite material are analyzed.

A method of predicting, theoretically, the compressive strength and failure modes of an idealized composite material is developed. The method is applied to a boron fiber/magnesium matrix composite and predicted strength values are compared to experimental data.

I. INTRODUCTION *

High modulus, high strength and lightweight filaments such as those made from quasi-amorphous boron (Refs. 1-3) have recently become available for consideration in the design and construction of advanced space structures. This provides the challenge to the structural designer to utilize the intrinsic mechanical properties of these materials to the fullest possible extent. It is necessary, however, to avoid misapplication caused by indiscriminate enthusiasm for the remarkable order-of-magnitude improvements in basic mechanical properties of these fibers compared to the more conventional materials of construction. Guidance in the search for fruitful avenues of development and structural design application can be derived from a careful study of the possibilities and limitations inherent in these new materials of construction.

For this purpose, it is necessary to provide some theoretical and experimental foundation in predicting the useful mechanical properties of filament composite materials from the known properties of its individual constituents. Considerable work has been published by several authors predicting elastic composite properties from those of the constituents (Refs. 4 , 5). A more difficult, but equally important task is to predict mechanical strength. The difficulty is primarily due to the fact that mechanical strength is a property

*This report is one phase of a study on Boron filament composite materials for space structures.

which is strongly affected by "accidents" such as premature modes of failure, micro-flaws, dislocation mobility (or the lack thereof), aging, manner of conducting the tests, etc.

In this study, an attempt is made to isolate the uniaxial compressive failure mechanisms of a simplified model for a composite material and to predict its ultimate compressive strength based solely upon the elastic and elasto-plastic properties of the constituents, and upon the geometry of the micro-structure in the composite material. Such predictions, supported by experimental evidence, can form the basis for generalized application studies such as presented in Refs. 6 and 7. These, in turn, will identify areas of worthwhile application and, ultimately, allow a realistic judgement regarding the relative cost effectiveness of new and necessarily expensive high performance composites as compared to alternate, more conventional methods and materials of construction.

II. COMPRESSIVE FAILURE IN UNIAXIAL LAMINATES

A. Micro-Stability Failure

A strongly idealized "two-dimensional" model of a uniaxial composite material as shown in Figure 1 will be considered. This model consists of alternating layers of a relatively soft matrix and a hard, load-carrying skeleton which is representative of a fiber reinforcement. We will assume that the skeletal constituent material is columnated, Hookean, and has unlimited compressive strength. We will further assume that the matrix has elasto-plastic properties and that its Young's modulus is small compared to that of the skeleton. The material will be subject to uniaxial compressive loading parallel to the direction of the reinforcement. Possible modes of materials failure, then, are those where the skeletal material will cripple elastically under applied axial loading (micro-stability failure).

For this idealized material, there are two possible micro-stability failure modes as shown in Figure 2. The first forms a pattern symmetrical to mid-planes through the matrix layers (Fig. 2a). This case represents a condition analogous to the well known case of the column on an elastic foundation (Refs. 8, 9). Disregarding Poisson's ratio effects in the matrix yields the crippling stress

$$F_{cr_{sym}} = \frac{2}{\sqrt{3}} E_m \alpha \sqrt{\frac{\alpha}{1-\alpha}} E_f/E_m \left[1 + \frac{1-\alpha}{\alpha} E_m/E_f \right] \qquad (1)$$

where the packing density $\alpha = \frac{w_f}{w_f + w_m}$ is the volumetric ratio of skeleton material to total composite material.

The second failure mode forms an antisymmetrical pattern as shown in Figure 2b. Here the matrix is primarily subject to shearing deformation. Considering only the contributions of axial skeletal stiffness and shear stiffness of the matrix, the method of minimum potential energy yields a crippling stress

$$F_{cr_{antis}} = \frac{G_m}{1 - \alpha} \tag{2}$$

Note that, subject to the limitations inherent in the underlying assumptions, the two crippling stresses are independent of the overall sample dimensions and dependent only of the micro-structure and constituent elastic materials properties characterized by α and $(E_f/E_m, G_m)$ respectively.

The stability analysis is made by assuming perfectly elastic properties of the two composite constituents. Subject to the limitations of small deformation analysis, the results can also be applied to the case where the matrix has exceeded the yield point due to axial compressive strains. This requires replacing the transverse Young's modulus and shear modulus of the matrix material with the appropriate tangent moduli, corresponding to the particular axial

compressive matrix strain in the material. The crucial assumption made here is that the material retains isotropy of its elastic properties in the post-yielded state.

Equating the two crippling stresses given in Equations (1) and (2) yields an expression for the boundary between the two failure domains as follows:

$$E_{f/E_m} = \left[\frac{16}{3}\left(1+\mu_m\right)^2 \left(1-\alpha\right)\alpha^3 \left(1+{}^{E_m}/_{E_f}\,\frac{1-\alpha}{\alpha}\right)^2\right]^{-1} \qquad (3)$$

The failure domains according to Equation (3) are shown in Figure 3 for a Poisson's ratio of $\mu_m = .5$ (plastic) and .3 (elastic). This graph shows, that for reasonably high packing densities $\alpha > .2$ and modulus ratios, ${}^{E_f}/_{E_m} > 5$, the antisymmetrical crippling mode will prevail. For this case, then, the compressive failure stress, $F_{c_{ult}}$, can be determined solely from the effective (tangent) shear modulus $\bar{G}_m$ and the packing density α by the relation given in Equation 2. As discussed below, in most cases the stability failure will take place at strain levels exceeding the yield point of the matrix material. Thus the point of failure will be determined by:

$$F_{c_{ult}} = \alpha\,\varepsilon\,E_f + (1-\alpha)\,f_m^* = \frac{\bar{G}_{m(\varepsilon)}}{1-\alpha} \qquad (4)$$

Here f_m^* is the stress carried in the matrix at failure and $\bar{G}_m(\varepsilon)$ is the tangent shear modulus of the matrix material as a function of axial strain ε. A graphical interpretation of Equation (4) is shown in Figure 4.

B. Limits of Elastic Stability Failure

Failure may take place in the fully elastic range or in a range where the matrix material has reached an elasto-plastic state. Let the composite modulus (Ref. 5) for a perfectly columnated composite:

$$E_c = \alpha E_f + (1-\alpha)\bar{E}_m \tag{5}$$

then, as seen from Figure 4, elastic failure will take place if

$$E_c \geq \frac{\bar{G}_{m_y}}{\varepsilon_{m_y}(1-\alpha)} \tag{6}$$

where $\bar{G}_{m_y}$ and ε_{m_y} are the tangent shear modulus and compressive strain at the matrix yield point respectively.

From Equations (5) and (6) we obtain as a criterion for elastic crippling

$$\varepsilon_{m_y} = \left\{2(1+\mu_{m_y})(1-\alpha)\alpha\left[E_f/E_m + \frac{1-\alpha}{\alpha}\right]\right\}^{-1} \tag{7}$$

For the case $\mu_{m_y} = .3$ and for several values of α, the relationship between ε_{m_y} and E_f/E_m is shown in Figure 5.

The location of a number of candidate composite constituents are shown in Figure 5. Mechanical properties that have been assumed for this purpose are listed below. Data have been obtained from References 10 and 11.

Skeleton:	E_f, 10^6 psi	
Boron	60	
S-Glass	12	
Matrix:	E_m, 10^6 psi	ε_{my}
Titanium	16	.75%
Aluminum	10.2	.3 %
Magnesium	6.5	.2 %
Epoxy	.5	2.5 %

Note that of the several composites considered only the Boron-Epoxy combination has sufficiently high yield strain and modulus ratio to exhibit elastic crippling. Thus, in composites using metallic matrix materials, anelastic crippling may be expected to limit the ultimate compressive strength.

This analysis also shows, that considerable improvements in compressive strength are available with matrix materials of moderate shear moduli and relatively high yield strains.

III. COMPRESSIVE STRENGTH OF BORON-MAGNESIUM COMPOSITES

A. Experimental

Composite materials samples have been prepared from boron fibers produced at ASTRO RESEARCH CORPORATION by infiltration with magnesium melts in a process similar to that described for boron-aluminum composite materials in previous work (Ref. 2). Figure 6 shows a side view, and Figure 7 shows a cross-section micrograph of a typical sample. Two test samples were subject to compression loads in increments of approximately 30,000 psi and at average loading rates of approximately 1000 psi/sec. In both cases, total failure was observed at compressive strains of approximately .7% to .8%. The failure appearance was that of a simultaneous crumbling of the test specimen along its total free length. A top view of the sample after complete failure is shown in Figure 8.

A third sample was subject to 3-point bending tests in the apparatus shown in Figure 9. Here, the failure appeared localized at the point of maximum stress and essentially without permanent deformation. Observation of the fracture appearance did not establish whether it was initiated at the compression or the tension side of the specimen.

Properties of the three samples and their experimentally determined failure stresses are as follows:

Test Sample	#1	#2	#3
Packing Density	.52	.71	.52
Length/Diameter (in)	.80/.13	.98/.25	2.0/.13
ρ Specific Weight lbs/in^3	.085	.093	.085
Type of Loading	Compr.	Compr.	Bending
$F_{c_{ULT}}$ Ultimate Composite Stress, 10^3 psi	188	349	199 *)
Ultimate Fiber Stress- 10^3 psi **)	342	486	363
$\frac{F_{c_{ULT}}}{\rho}$ Specific Strength of Composite, 10^6 psi	2.21	3.75	2.34

For the purpose of comparison, the specific strength values for a number of typical isotropic high grade structural materials are given below.

	$F_{c_{ULT}}$ 10^3 psi	ρ lbs/in^3	$F_{c_{ULT}}/\rho$ 10^6 in
High Strength Alloy Steel	300	.285	1.05
Aluminum Alloy	75	.10	.75
Titanium	200	.15	1.33
Berillium	90	.066	1.35
Magnesium	30	.065	.46

B. Analysis

For the case of a boron/magnesium composite, the anelastic crippling failure has been evaluated according to the shear crippling theory for the simplified composite model discussed in Section II. Figure 10 shows the post-yielding shear modulus $\bar{G}_m$ of magnesium in function of normal strain, computed from stress-strain curves given in Reference [10]. Also in Figure 10 is shown the scaled stress-strain curve for the boron/magnesium composite, for two typical packing densities . It can be seen that the matrix material will exceed the yield point at stress levels of approximately 25% to 30% of the ultimate strength of the composite.

Ultimate composite stress Fc_{ult} and strain, ε_{ult}, at failure are plotted in function of packing density in Figure 11. Experimental values obtained from the three samples are also shown. In view of the relatively crude analysis and the very limited experimental data, the correlation obtained between theoretical prediction and experimental data appears remarkable and, perhaps, fortuitous. Nevertheless, some hope is generated that the approach outlined in this report may bear fruit in identifying the critical composite materials parameters and in providing analytical tools for quantitative prediction of significantly improved mechanical properties.

IV. CONCLUSIONS

Metal matrix-boron fiber composite materials can be made that exhibit specific strength values considerably above those available in monolithic materials. Limited test data indicate that anelastic micro-stability failure analysis yields theoretical strength predictions which are reproduced in experiments. The high modulus of the reinforcing boron fiber allows the design of very efficient compression resistant structural elements (such as truss columns), which can exploit the available high specific strength of the composite materials.

An important characteristic of these materials is the fact that yielding in the ductile matrix will occur at small fractions of the ultimate failure stress. As a consequence, the use of their high stress level capacity in applications requiring repeated loading has to be viewed with care. "Single shot" missile applications would appear to constitute first contenders for practical applications, until the fatigue characteristics of those materials are well established.

Finally, the use of a castable metallic matrix allows a design freedom at attachment and interface structures which is not available with the more conventional glass-resin fiber composites. It can be expected, therefore, that the boron-metal composite materials will find practical applications in areas formerly reserved to conventional metal construction.

REFERENCES

1. Talley, C. P., et al: "Boron Reinforcements for Structural Composites", ASD-TDR-62-257, March 15, 1962.

2. Witucki, R. M.: "Boron Filaments", NASA CR-96, September 1964.

3. Berry, J.: "Preliminary Mechanical Properties of High Modulus Filaments" (U), General Electric Company, February 1964 (Confidential

4. Rosen, B. W., Dow, N. F., Hashin, Z.: "Mechanical Properties of Fibrous Composites", NASA CR-31, April 1964.

5. Tsai, S. W.: "Structural Behavior of Composite Materials", NASA CR-71, July 1964.

6. Micks, W. R.: "A Review and Evaluation of Filament-Composite Materials" (U), Memorandum RM-4168-PR, The RAND Corporation, October 1964 (Confidential).

7. Dow, N. F., Rosen, B. W.: "Evaluations of Filament-Reinforced Composites for Aerospace Structural Applications," Annual Report, Contract NASw-817, October 1964.

8. Timoshenko, S.: "Theory of Elastic Stability", McGraw-Hill, New York, 1936.

9. Pfluger, A.: "Stabilitaets Probleme der Elastostatik", Springer-Berlin, 1950.

10. "Materials Manual", Aerophysics Development Corporation, 1957.

11. "Metals Handbook", Vol. I, Am. Soc. Metals, 1961.

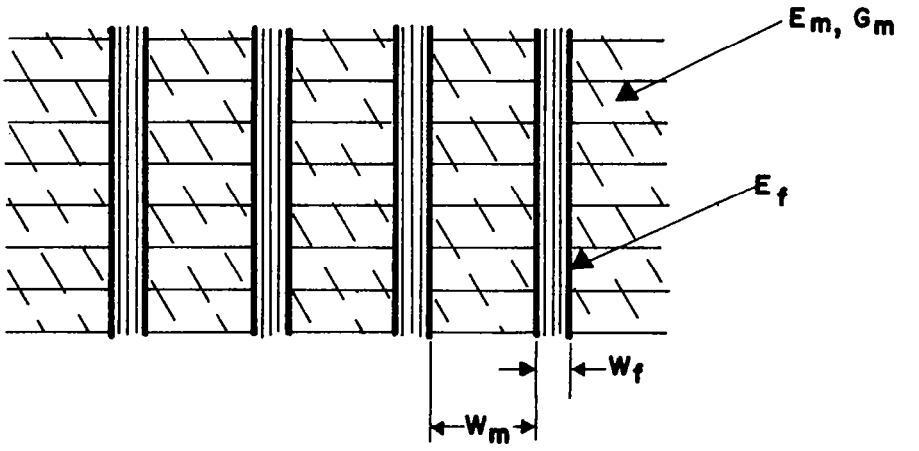

Figure 1

Idealized Composite Geometry

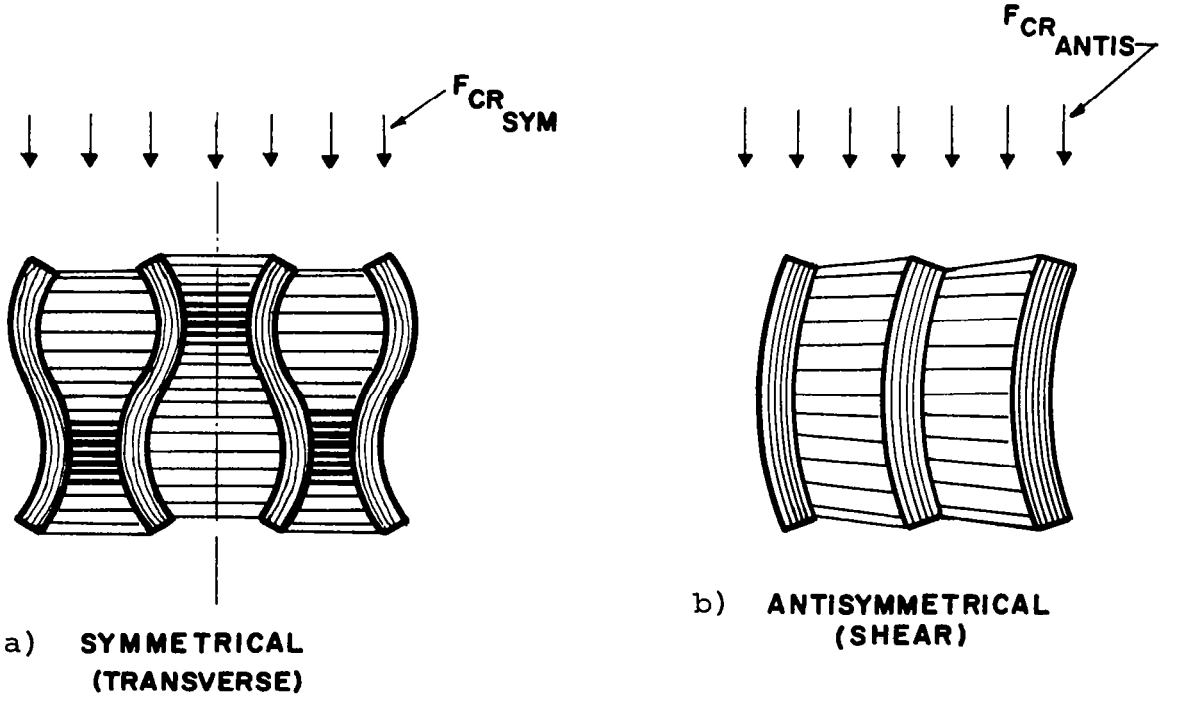

Figure 2

Micro-Stability Failure Modes

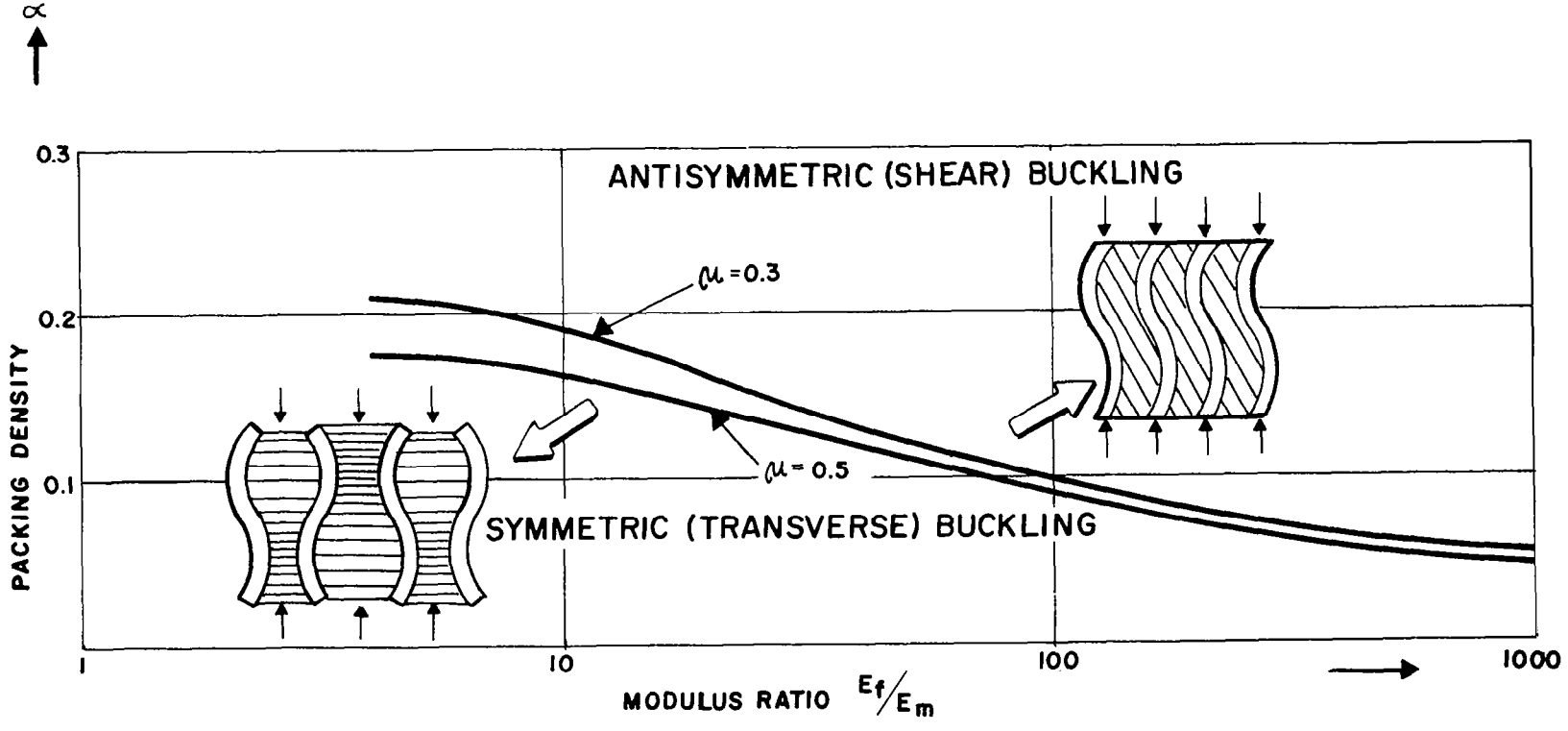

Figure 3

Micro-Stability Failure Domains

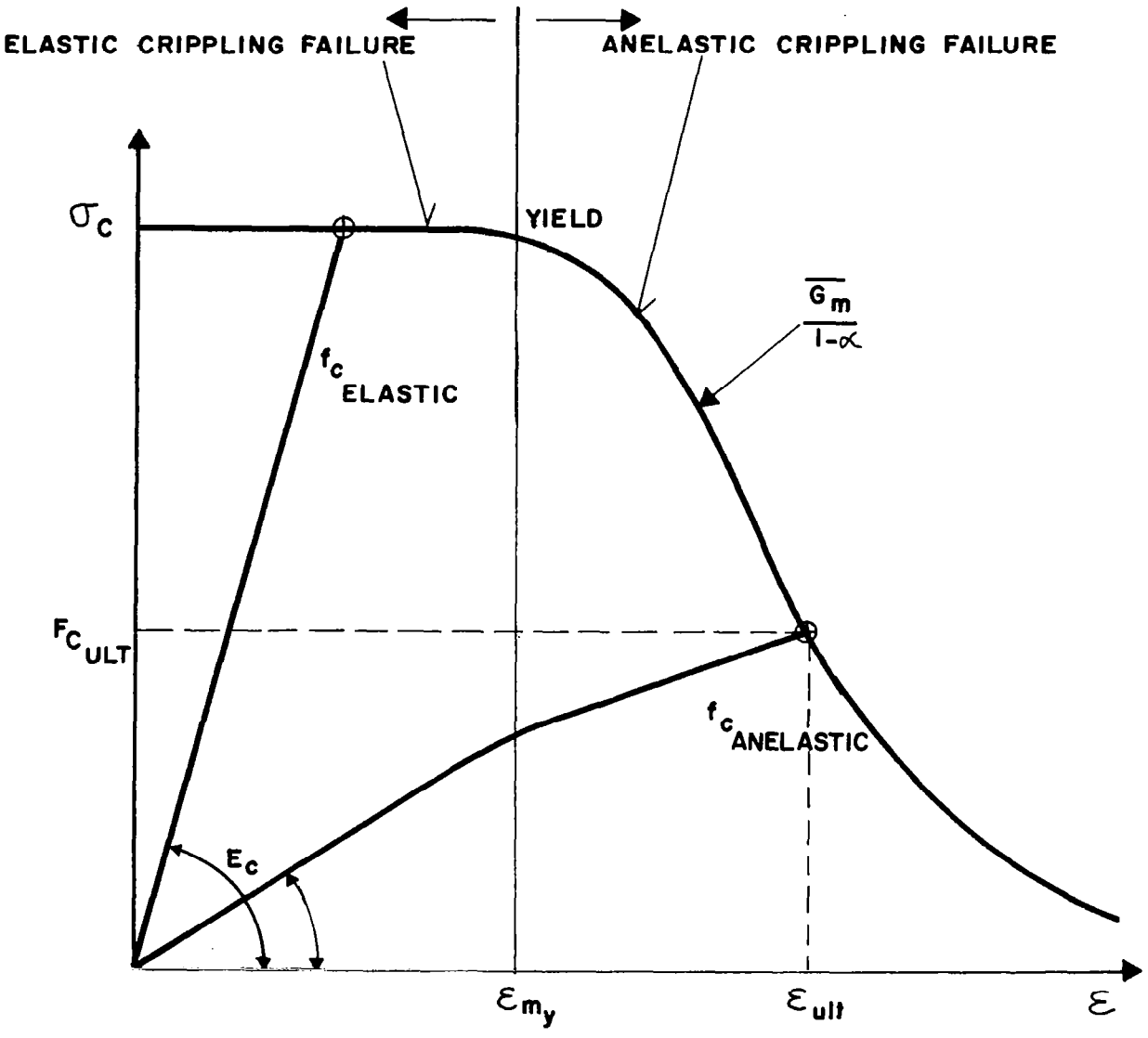

Figure 4

Composite Stress-Strain Limits

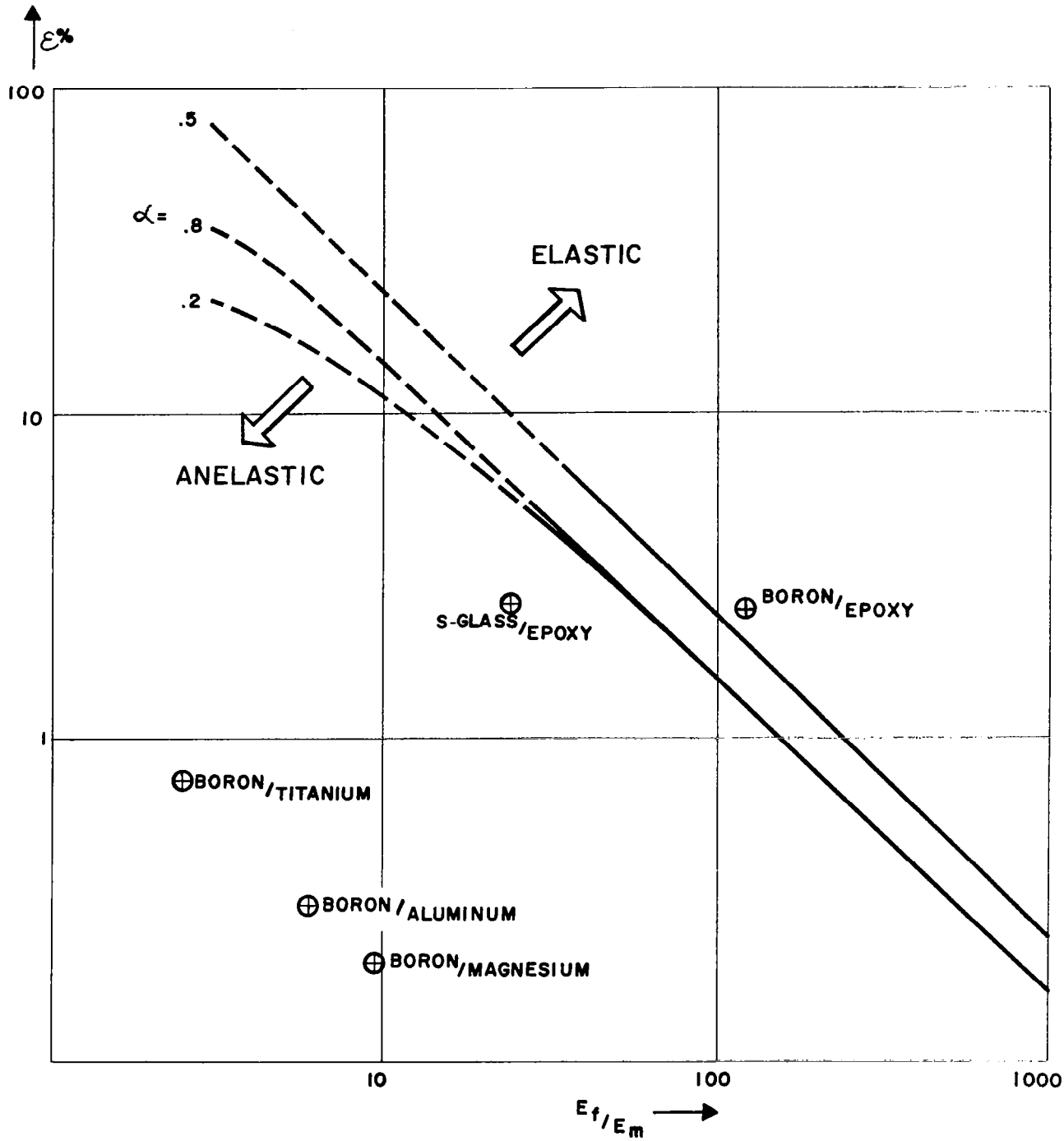

Figure 5

Anelastic and Elastic Shear Crippling Failure Domains

Figure 6

B/Mg Compression Test
Sample - Side View

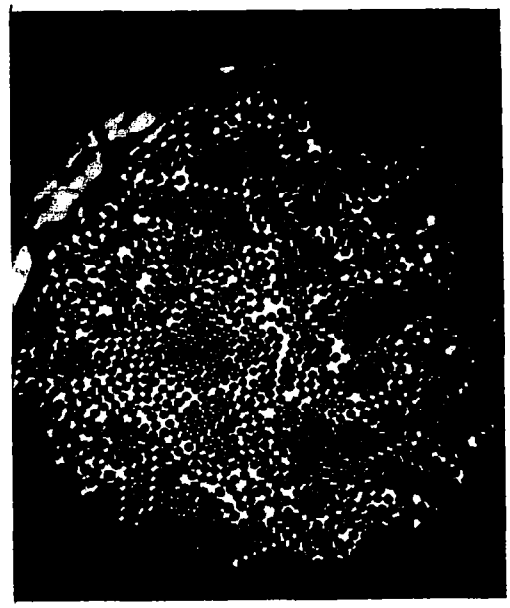

Figure 7

B/Mg Compression Test
Sample - α = .71 -
Partial Cross-section
Microphotograph 10 x
Linear Magnification

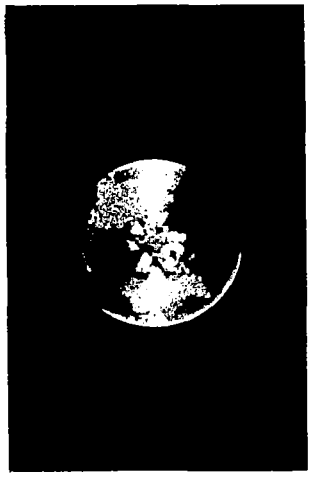

Figure 8

B/Mg Compression Test
Sample - Top View After
Failure

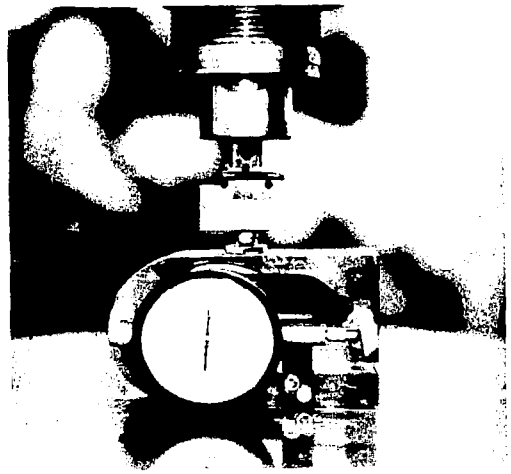

Figure 9

3-Point Bending Test
Set-up

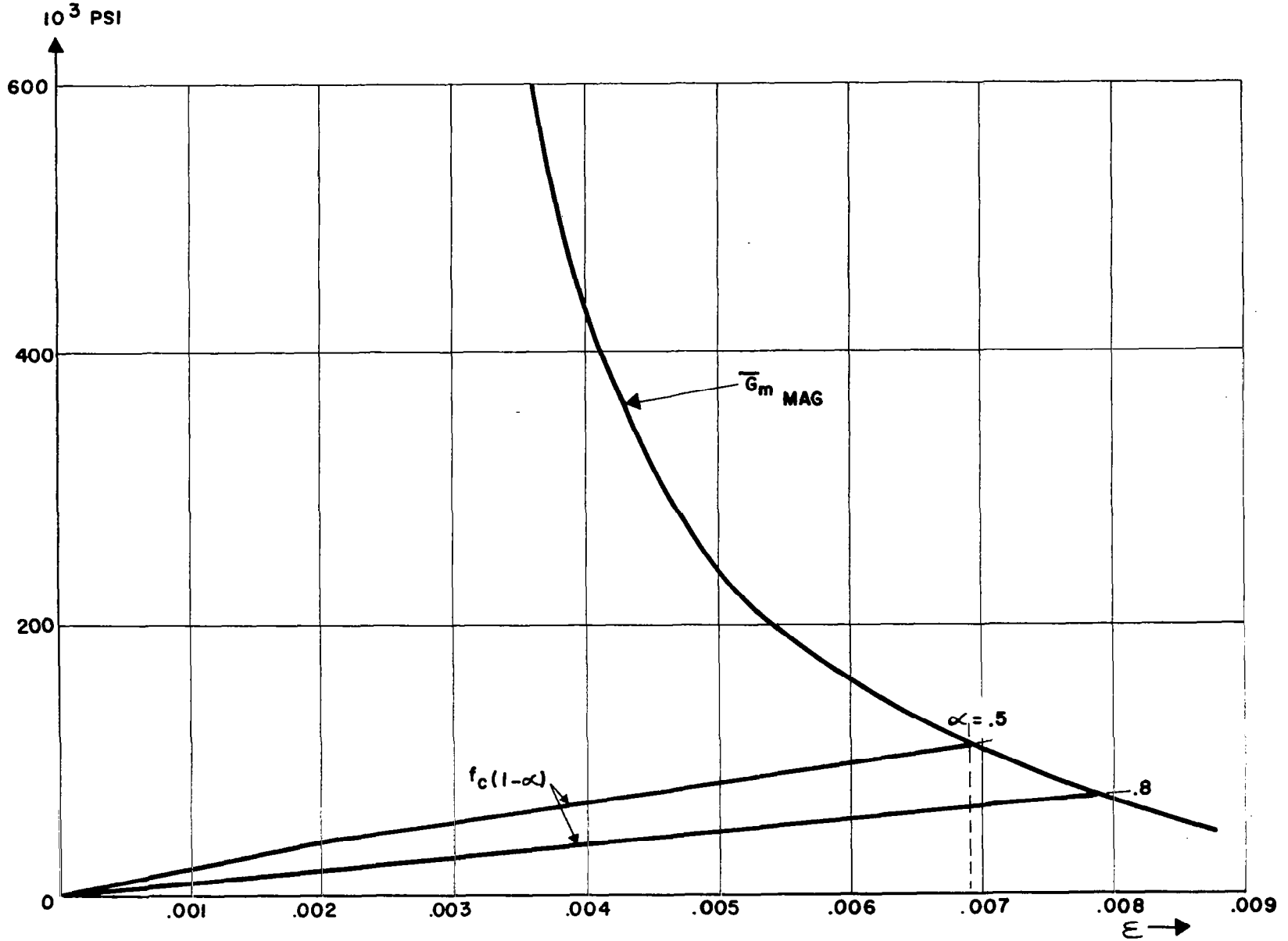

Figure 10

Tangent Shear Modulus for Magnesium and Composite Stress vs Strain

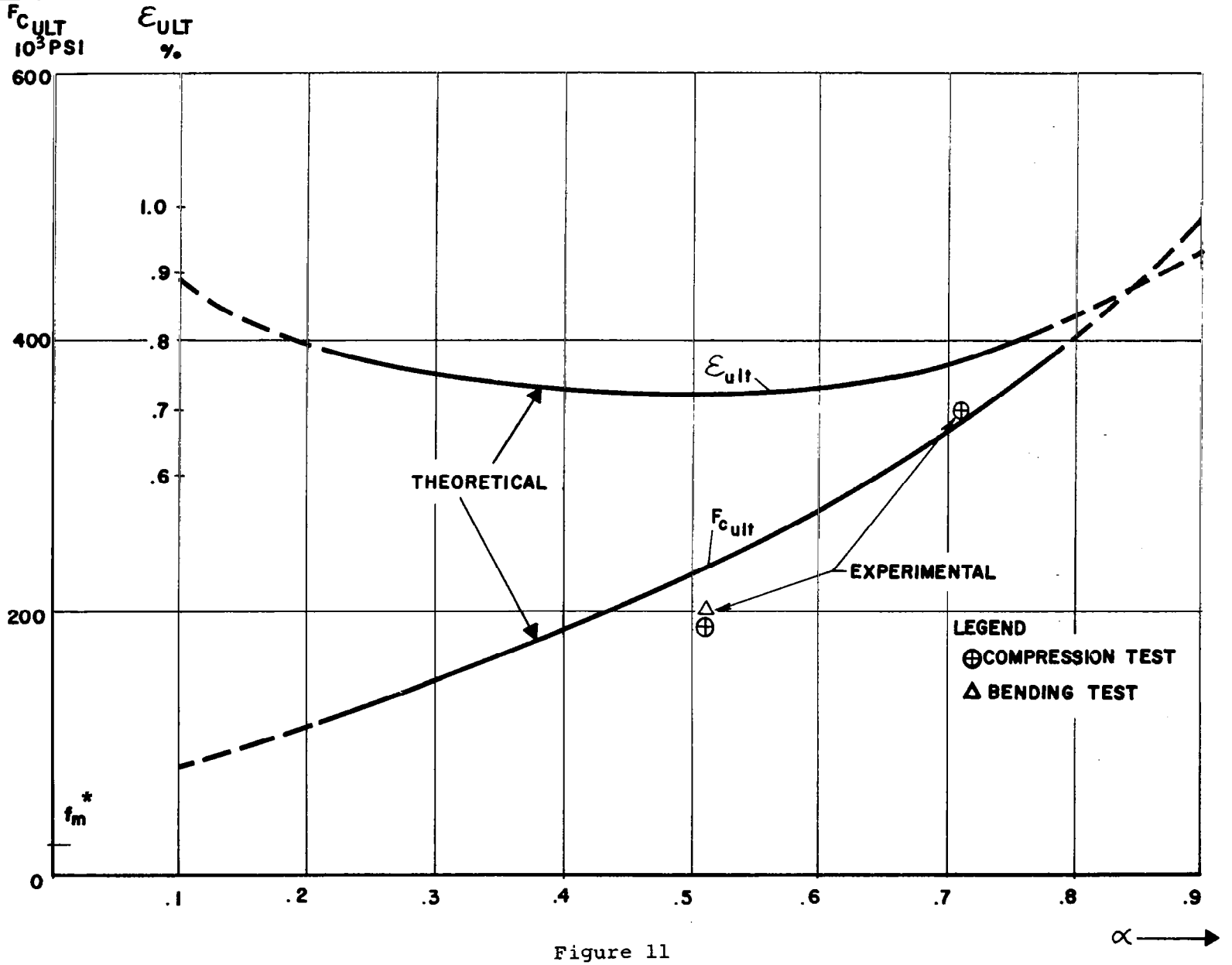

Figure 11

B/Mg Composite - Predicted and Experimental Compressive Strength vs Packing Density